⌘ *Author's Choice*

Soluble Amyloid Precursor Protein Induces Rapid Neural Differentiation of Human Embryonic Stem Cells*[S]

Kristine K. Freude, Mahmud Penjwini, Joy L. Davis, Frank M. LaFerla[1], and Mathew Blurton-Jones[2]

From the Department of Neurobiology and Behavior and Institute for Memory Impairments and Neurological Disorders, University of California, Irvine, California 92697

Human embryonic stem cells (hESCs) offer tremendous potential for not only treating neurological disorders but also for their ability to serve as vital reagents to model and investigate human disease. To further our understanding of a key protein involved in Alzheimer disease pathogenesis, we stably overexpressed amyloid precursor protein (APP) in hESCs. Remarkably, we found that APP overexpression in hESCs caused a rapid and robust differentiation of pluripotent stem cells toward a neural fate. Despite maintenance in standard hESC media, up to 80% of cells expressed the neural stem cell marker nestin, and 65% exhibited the more mature neural marker β-3 tubulin within just 5 days of passaging. To elucidate the mechanism underlying the effects of APP on neural differentiation, we examined the proteolysis of APP and performed both gain of function and loss of function experiments. Taken together, our results demonstrate that the N-terminal secreted soluble forms of APP (in particular sAPPβ) robustly drive neural differentiation of hESCs. Our findings not only reveal a novel and intriguing role for APP in neural lineage commitment but also identify a straightforward and rapid approach to generate large numbers of neurons from human embryonic stem cells. These novel APP-hESC lines represent a valuable tool to investigate the potential role of APP in development and neurodegeneration and allow for insights into physiological functions of this protein.

Alzheimer disease (AD)[3] is the leading cause of age-related dementia and is characterized by an irreversible loss of neurons accompanied by the accumulation of two hallmark pathologies: amyloid plaques and neurofibrillary tangles (1). A great deal has been learned about the genesis and biophysical role of β-amyloid (Aβ) in AD, and it is widely held that the accumulation of toxic oligomeric and fibrillar assemblies of Aβ are the major initiating factor in the development and progression of this disorder (reviewed in Ref. 2). Aβ is itself produced via the sequential proteolytic cleavage of a type-1 transmembrane protein called amyloid precursor protein (APP).

Emerging evidence suggests that APP may be involved in the development of the central nervous system. Knockout models of APP and its homologues, for example, exhibit lissencephaly, and *in utero* knockdown of APP leads to neuronal migration defects (3, 4). It was also recently shown that APP is expressed in human embryonic stem cells (hESCs) and suggested that a shift in APP proteolysis may modulate hESC self-renewal and differentiation (5). To further investigate the potential role that APP plays in hESC fate, we generated hESC lines that stably overexpress APP. These lines may provide a novel human-based cellular model of AD. In addition, we find that these APP-hESC lines provide a fascinating approach to study the marked influence of APP proteolysis on neuronal differentiation.

To study the influence of APP cleavage products on hESC differentiation, it is important to understand the mechanisms by which these various products are generated (reviewed in Ref. 6). Aβ, for example, is produced via the sequential proteolytic cleavage of APP, which is first cleaved by the β-secretase enzyme BACE-1, releasing a soluble fragment, sAPPβ, into the extracellular space. The remaining membrane-bound C-terminal APP stub (C99) is subsequently cleaved by γ-secretase, releasing the Aβ peptide and the APP intracellular domain, a signal peptide that may regulate specific gene transcription (reviewed in Ref. 7). APP is also more commonly cleaved via the non-amyloidogenic pathway, whereby α-secretase (ADAM10 or ADAM17)-mediated cleavage occurs within the Aβ sequence, precluding Aβ generation. The non-amyloidogenic processing of APP also leads to the extracellular release of a soluble fragment (sAPPα) and, following γ-cleavage, the release of AICD. Interestingly, a number of studies suggest that sAPPα, can exhibit trophic-like activity. For example, sAPPα has been implicated in neurite outgrowth, neuroprotection, neurotrophism, adult neurogenesis, axonal transport, synaptic function, and transcriptional regulation (8–15). Thus, sAPPα appears to be a critical factor in neuronal maintenance and growth. In contrast, the potential role of the slightly shorter sAPPβ has been largely unexplored.

Here we show that all APP-overexpressing hESC clones rapidly differentiate toward a neuronal fate without the need for

[S] The on-line version of this article (available at http://www.jbc.org) contains supplemental Figs. 1–4.

⌘ *Author's Choice*—Final version full access.

[1] To whom correspondence may be addressed: Dept. of Neurobiology and Behavior, University of California, Irvine, Irvine, CA 92697-4545. E-mail: laferla@uci.edu.

[2] To whom correspondence may be addressed: Dept. of Neurobiology and Behavior, University of California, Irvine, Irvine, CA 92697-4545. E-mail: mblurton@uci.edu.

[3] The abbreviations used are: AD, Alzheimer disease; Aβ, β-amyloid; APP, amyloid precursor protein; sAPPβ, secreted amyloid precursor protein beta; hESC, human embryonic stem cell; TUJ, β-3 tubulin; qPCR, quantitative PCR; ANOVA, analysis of variance; ZO-1, zona occludens protein 1; PS, presenilin.

exogenous factors. We generated APP-hESC lines expressing either wild-type APP or APP carrying the Swedish mutation (KM670/671NL). The Swedish mutation occurs adjacent to the β-secretase cleavage site, promoting the amyloidogenic cleavage of APP and increasing Aβ generation (16). Robust differentiation in these APP-hESC lines is apparent as early as 4 days following manual passaging, despite maintenance in standard hESC conditions that reliably maintain untransduced and control transfected hESCs. To investigate the mechanism by which APP drives neuronal differentiation, we examined the levels of α-, β-, and γ-secretase components and examined the influence of various APP cleavage products on hESC differentiation. Our findings point to a specific role for APP in development of the neuronal lineage, in which a fine balance of APP proteolysis can modulate self-renewal *versus* differentiation. Our data also clearly demonstrate that both sAPPα and sAPPβ can alone drive rapid and robust neural differentiation of hESCs. Our studies therefore reveal a novel and straightforward approach to rapidly generate large numbers of neural precursor and neurons from hESCs within 4–7 days.

MATERIALS AND METHODS

Lentiviral Vector Constructs—To generate wild-type and mutant APP lentiviral constructs, we used the ViraPower™ lentiviral expression system (Invitrogen). For all constructs, the 695-amino acid form of human APP was used, as it represents the most abundant isoform within the brain (17). Wild-type or Swedish mutant (KM670/671NL) APP cDNA sequences were amplified by PCR and cloned into the pENTR plasmid via TOPO® cloning.

To better mimic the physiological regulation of APP expression, we utilized the human APP proximal promoter to drive transgene expression. The 1.2-kb APP proximal promoter sequence spanning the transcriptional start site and including the minimum region driving basal promoter activity was kindly provided by Dr. Debomoy Lahiri (18) and was cloned into the pENTR-5- entry clone by TOPO® cloning. The resulting hAPP pENT™5′-promoter clone was then combined with the various pENTR-APP clones using the Multiside Gateway® LR recombination reaction. Plasmids were sequenced, and lentiviral particles were subsequently generated by the University of California Los Angeles Molecular Vector Core.

Generation of Stable APP-hESC Clones—WA09 (H9) hESCs from WiCell (WI) and HUES7 hESCs from Dr. Douglas A. Melton (Harvard) were grown on Matrigel (BD Biosciences) using mTeSR® medium (Stemcell Technologies, Palo Alto, CA) and manually passaged every 4–5 days. H9 cells (P35) and HUES7 cells (P27) were grown on blasticidin-resistant mouse embryonic feeder cells (Invivogen, San Diego CA) and then transduced with APP lentiviral particles using the ViraDuctin™ lentivirus transduction kit (Cell Biolabs, San Diego, CA). Media were changed 12 h later. Cultures were maintained in mTeSR media until small hESC colonies were established. Blasticidin (0.5 μg/ml, Invivogen) was then added to select for stably transduced clones. Cultures were maintained and passaged in mTeSR with blasticidin for 30 days, and then stably transduced hESC clones were picked and expanded. All lines were grown after the selection process under identical, hESC-optimized

conditions using mTeSR growth media, Matrigel-coated culture dishes, and strict manual passaging. This method of stem cell culture maintenance ensures a very high proportion of undifferentiated cells in untransduced and control-transfected H9 and HUES7 lines, with only rare differentiating cells observed at the edges of the colonies.

Recombinant Protein Treatment—H9 cells were grown in mTeSR medium in 24-well plates coated with Matrigel and treated for 5 days with 0 nM, 1 nM, 10 nM, or 100 nM recombinant human sAPPα or β (Sigma). Each treatment group consisted of three wells with at least eight hESC colonies at the beginning of treatment. Media and peptide were replaced each day, and after 5 days of treatment, cells were fixed with 4% paraformaldehyde and analyzed by immunofluorescence.

Western Blotting and ELISA—Cells were washed, lysed in M-PER® mammalian protein extraction reagent (Pierce) with protease inhibitors (Sigma), and sonicated. Equal amounts of total protein were separated by SDS-PAGE, electrotransferred using Invitrogen iBlot, probed with appropriate antibodies, and visualized with Super Signal West Dura (Thermo Scientific, Waltham MA). Band intensity was quantified in ImageJ and normalized to GAPDH. Primary antibodies used were PS1 (Novus, Saint Louis, MO), PS2, nicastrin (Cell Signaling Technology, Inc., Danvers, MA), APP/22C11, Adam10 (Millipore, Billerica, MA), BACE1, CT20, ADAM17 (Calbiochem/EMD4 Bioscience, Gibbstown, NJ), and GAPDH (Santa Cruz Biotechnology, Santa Cruz, CA).

sAPPα and β Immunoprecipitation—Media were collected and concentrated using Amico Ultra 15-ml 30-kDa centrifugal filters (Millipore). sAPPα and β were then immunoprecipitated with 22C11 and protein G-agarose (Roche) following standard protocols. Bound proteins were then processed for Western blotting and probed with sAPPα- and sAPPβ- specific polyclonal antibodies (Covance-Signet, Princeton, NJ). Secreted Aβ was measured using a sensitive sandwich ELISA (Wako Chemicals, Richmond, VA).

Immunohistochemistry—Cells were fixed in 4% paraformaldehyde, blocked with 10% normal goat serum, and incubated overnight (4 °C) with primary antibody followed by Alexa Fluor secondary antibodies and counterstained with DAPI. Primary antibodies included the following: Pax6 and APP (Covance), GFAP and tau (Dako, Glostrup, Denmark), β-3 tubulin (TUJ) (Millipore and Covance), nestin and APP (22C11) (Millipore), Tbr2 (Abcam, Cambridge, UK), and ZO-1 (Invitrogen). Images were captured using a Nikon Eclipse TI microscope, and figures were arranged in Photoshop CS2 (Adobe Systems). In some cases, image brightness and contrast were slightly adjusted.

Quantification of Neural Differentiation—For each comparison, six fields from three independent wells were captured using a Nikon Eclipse TI microscope, NIS-Elements AR 3.0 software (Nikon, Shinyuku, Tokyo, Japan), and a 10× objective. Total number of APP, nestin, or TUJ immunoreactive cells and DAPI-labeled nuclei in each image were then quantified by a blinded observer. For each field, APP, nestin, or TUJ counts were normalized to DAPI cell numbers to calculate the percent of differentiated cells. The values from all six fields were then averaged for each well. Average percent values for each condi-

tion were then compared statistically by Student's t test (Minitab v. 15) with the significance set to $p < 0.05$.

Real-Time Quantitative RT-PCR—RNA was prepared (RNA Minikit, Qiagen) and reverse transcribed with SuperScriptIII (Invitrogen). Q-PCR's were performed using the iScript SYBR green mixture (Bio-Rad) on the Bio-Rad MyiQ machine. All primers were obtained from Origene (Rockville, MD).

RESULTS

Generation and Analysis of APP-overexpressing Embryonic Stem Cell Lines—We generated APP-overexpressing hESC lines by lentiviral transduction of the H9 and HUES7 stem cell lines. Lentiviral constructs were generated to express wild-type APP or APP with the Swedish (Swe) mutation (KM670/671NL) under the control of the endogenous human APP proximal promoter (18). H9 and HUES7 hESC lines were transduced, and several stably transfected clones were selected and expanded. Two H9 clones, wild-type #9 (H9 APP WT) and Swedish #2 (H9 APP Swe), were used for further analyses and studies. Both lines showed significantly elevated levels of APP mRNA, exhibiting 190% (H9 APP WT) and 240% (H9 APP Swe) higher levels than control H9 cells by qPCR (ANOVA, $p < 0.001$) (Fig. 1A). More importantly, APP protein levels were also elevated by 190% (H9 APP WT) and 230% (H9 APP Swe) *versus* H9 control cells (ANOVA, $p < 0.001$) (Fig. 1, B and C). The observed increases in APP mRNA and protein expression confirm that it is possible to successfully generate hESC lines overexpressing mutant and wild-type forms of APP and indicate that the APP proximal promoter is active in hESCs.

APP-overexpressing hESC Lines Spontaneously and Rapidly Differentiate—All hESC lines were maintained and expanded on Matrigel using standard ESC conditions, mTeSR® media, and manual passaging. Control transduced and untransduced hESC lines exhibited typical healthy hESC colony morphology (Fig. 1D). In contrast, APP-overexpressing clones exhibited unusual colony morphology suggestive of significant spontaneous differentiation (Fig. 1E). Upon further examination, small circular arrangements of cells that closely resembled neural rosettes were readily apparent under phase contrast microscopy (Figs. 1F and 2, A–D). Neural rosettes typically only develop in hESC cultures when strong neural inducers such as retinoic acid are used to drive neural differentiation. In contrast, the observed phenotype occurred spontaneously in all APP clones regardless of whether they expressed mutant or wild-type APP constructs or whether they were derived from H9 or HUES7 lines. Importantly, this kind of differentiation was never observed in H9, HUES7, or control-transduced hESC lines grown under the exact same conditions. Thus, the observed phenotype appears to be dependent on APP expression. In addition to the appearance of small rosette-like structures, about 50% of the APP stem cell colonies developed much larger tubular structures (Fig. 1E) that were completely absent in H9 control embryonic stem colonies (D).

To exclude the possibility that major chromosomal rearrangements or anaploidy might contribute to the differentiation phenotype, counts of metaphase chromosomes were performed for several APP-hESC clones. All of the clones investigated had a normal karyotype of 46, XX (H9-derived clones, Fig. 1G) or 46, XY (Hues7-derived clones). Spontaneous differentiation is therefore caused by APP overexpression and not by chromosomal rearrangements.

Next, we examined the expression of two standard markers of pluripotency, Oct-4 and SSEA4. As expected, control H9 colonies exhibited strong expression of both markers (Fig. 1, H and I). Recently passaged APP-hESC clones also expressed both Oct-4 and SSEA4 (Fig. 1, J and K). However, Oct-4- and SSEA4-negative patches of cell were readily observed within APP-ESC colonies providing further evidence of spontaneous differentiation (Fig. 1, J and K, *blue* only). To further examine the expression of APP in control and APP-expressing hESC, we performed immunohistochemical analysis and quantification. In line with our Western blot analysis data, ~20% of control H9 cells express APP, albeit at low levels (Fig. 1, L and N). In contrast, strong APP expression is detected in over 80% of APP-hESCs (Fig. 1, M and N).

Overexpression of APP Preferentially Drives Neural Differentiation—The striking morphological resemblance of the small circular structures to neural rosettes led us to investigate whether these cells expressed markers of neural lineage commitment. Neural rosettes are the developmental signature of neural progenitors in cultures of differentiating stem cells, and the rosettes themselves are radial arrangements of columnar cells that express many of the proteins produced by neuroepithelial cells within the developing neural tube. In addition to similar morphology, neural progenitors within rosettes can, like the cells in the neural tube, further differentiate into the three principal cell types of the CNS: neurons, oligodendrocytes, and astrocytes.

Quantification of immunofluorescently labeled APP-hESC clones revealed that a great majority of cells within these cultures expressed the neural progenitor marker nestin within just 5 days of manual passaging (Fig. 2A, E, and Z). About 80–85% of these cells, regardless of whether mutant or wild-type APP was overexpressed, were nestin-positive, whereas only 2% of the H9 cells grown under exact conditions were nestin-positive (Fig. 2, I and Z). This increased nestin immunoreactivity within APP clones was highly significant and represented a more than 40-fold induction (ANOVA, $p < 0.001$). Interestingly, there was no significant difference in the degree of nestin expression between the different wild-type and mutant APP-ESC clones (ANOVA, $p = 0.64$) (Fig. 2Z). To further examine the nature of these rosette-like structures, we labeled cultures with the marker zona occludens protein 1 (ZO-1), which outlined a small inner lumen that is typically observed in ESC-derived neural rosettes (Fig. 2, C and G). ZO-1 is a phosphoprotein associated with tight junctions, which are important later in mature neurons, and establishes polarization of epithelial cells and creates diffusion barriers to paracellular passage (19). In addition to expressing nestin and the presence of ZO-1-outlined inner lumens, the cells within these neural rosettes also express the transcription factor Pax6 (Fig. 2, M and P). Pax6 is an early neural progenitor cell marker that is thought to modulate Sox2 expression (20). Expression of T-brain gene-2 (Tbr2), a marker of the intermediate (basal) progenitor cells of the developing cerebral cortex, was also detected in these cultures (Fig. 3, I and J) (21). Taken together, our data clearly dem-
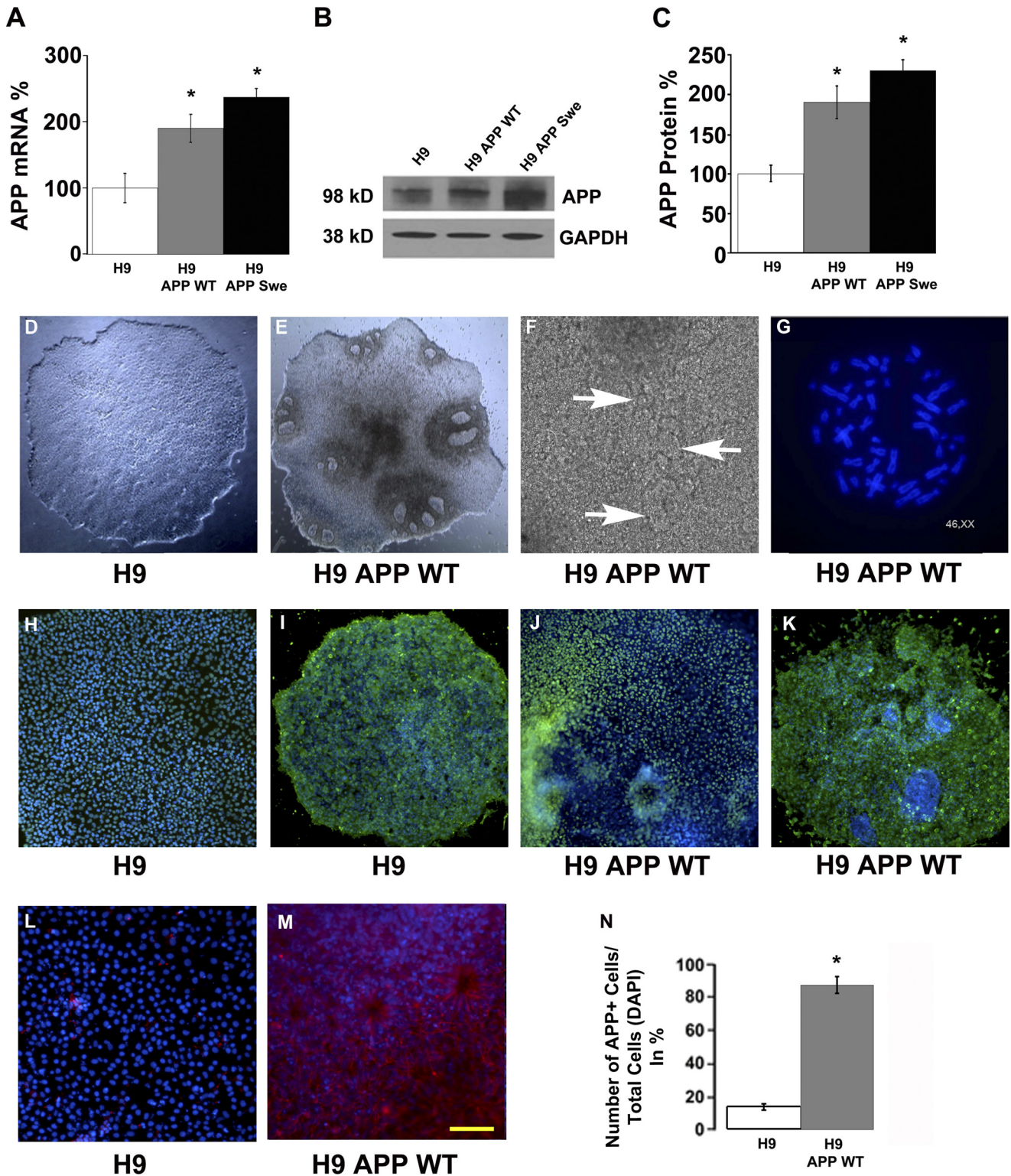
FIGURE 1. **Overexpression of APP markedly alters the morphology of hESC colonies.** *A*, qRT-PCR shows that APP mRNA is significantly elevated in the H9 APP WT and H9 APP Swe clones compared with the parental cell line. APP mRNA was 190 and 240% higher than in untransfected cells. *B* and *C*, likewise, APP protein levels were 190 and 230% higher in the APP WT and mutant clones, respectively. *D*, H9 control colonies display typical densely packed hESC colony morphology, whereas APP-ES clones (H9 APP WT line shown) exhibit large tubular structures and smaller rosette-like morphology (*E*). *F*, higher-power image of rosette-like structures in APP-ES clones. *G*, importantly, karyotype analysis reveals no major chromosomal changes in any of the APP-expressing lines (the H9 APP WT line is shown). *H* and *I*, pluripotency markers Oct-4 and SSEA4 confirm the undifferentiated status of H9 control cells. *J* and *K*, newly passaged APP-ES clones also exhibit Oct-4 and SSEA4 pluripotent cells (*green*). However, Oct4 and SSEA4 negative regions (*blue* only) are also observed within APP-ES colonies as spontaneous differentiation rapidly proceeds. *L*, low levels of APP (*red*) are detected in H9 control cells. *M*, in contrast, APP-ES clones exhibit elevated APP immunoreactivity (*red*). *N*, cell counts reveal that 17–20% of H9 control cells express low levels of APP, whereas 80–90% of APP-hESCs express this protein (*, $p < 0.05$). *Scale bar* = 300 μm (*D, E, I,* and *K*), 180 μm (*H* and *J*), and 100 μm (*F, L,* and *M*).

onstrate that APP-overexpressing stem cell clones spontane-
ously and rapidly differentiate to express early neural markers
within 80–85% of the cells.

Next we examined TUJ, an intermediate marker of neuronal
differentiation expressed in late-stage neuronal progenitor cells
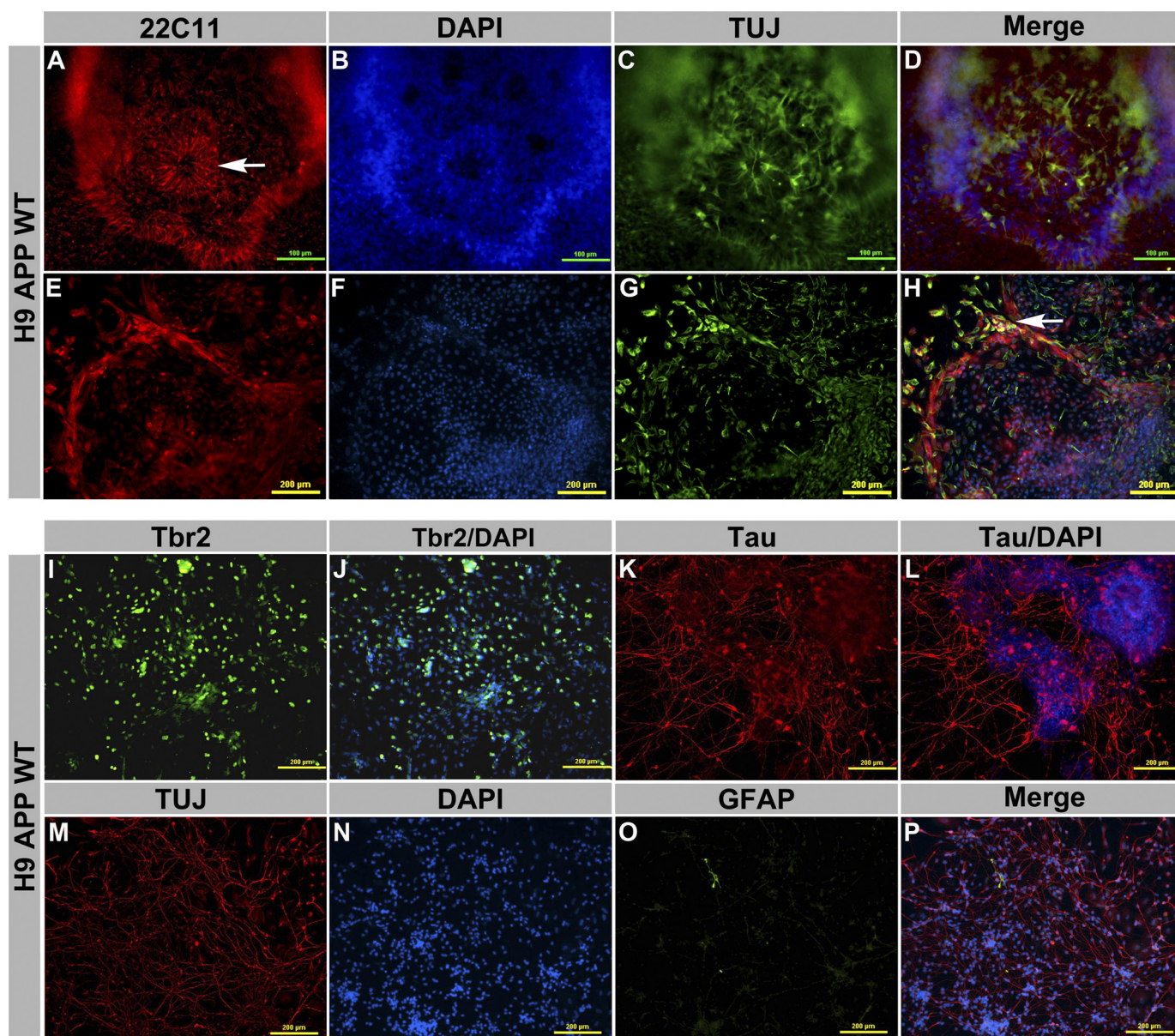and mature neurons. As expected, H9 control cells showed no
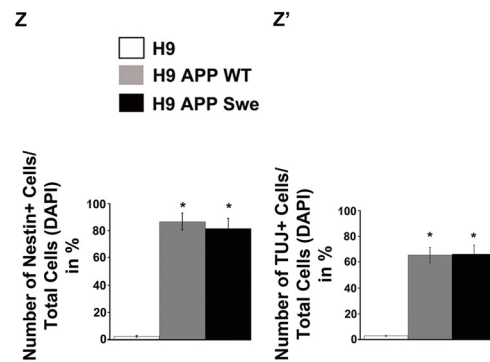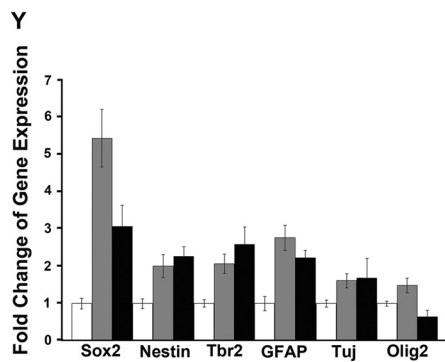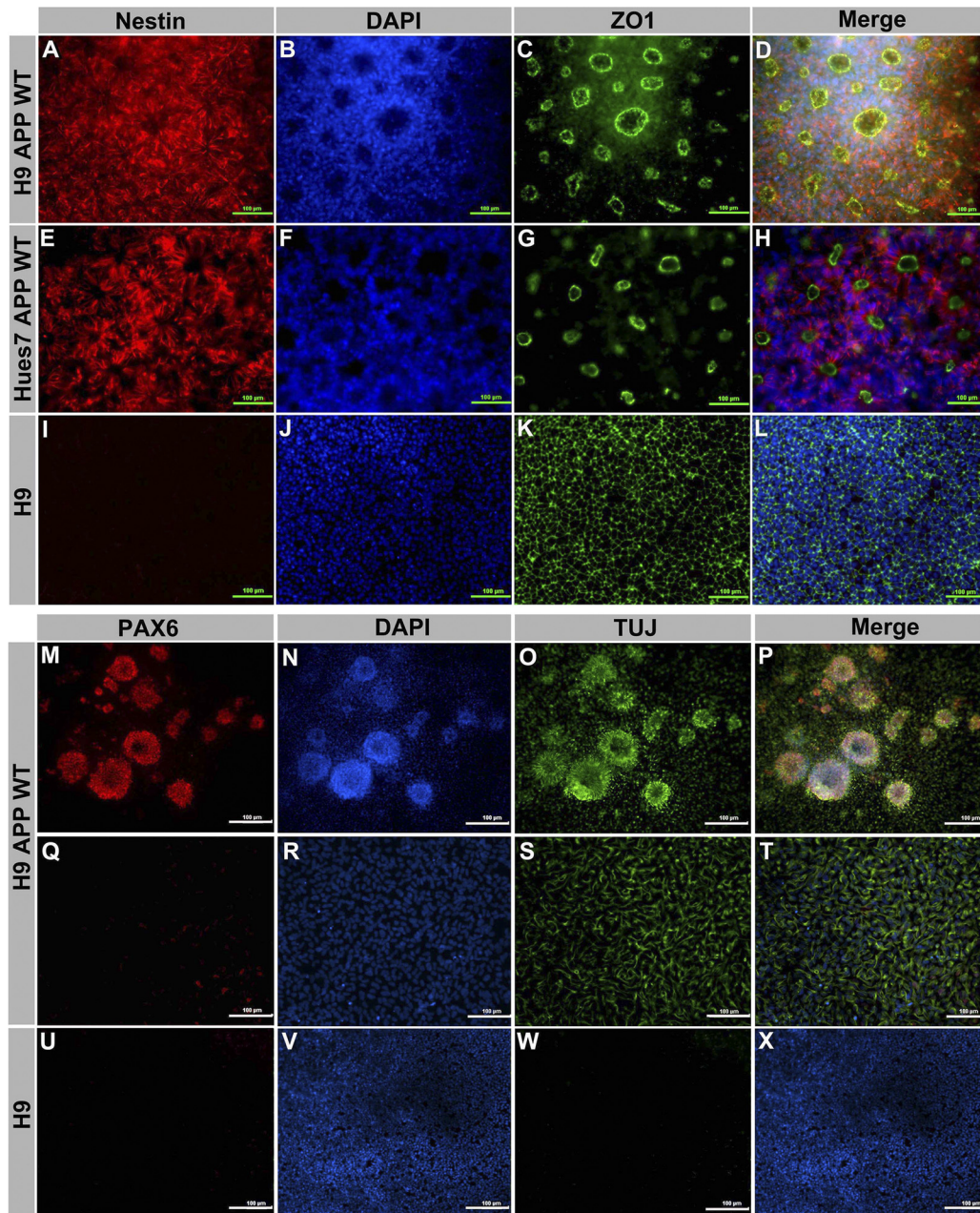
FIGURE 3. **Mature neural markers and neurite outgrowth are rapidly induced by APP overexpression.** *A–H*, H9APP WT clones robustly express APP (*red*) which is often observed in association with rosette-like structures (*A, arrow*) or TUJ+ cells (*green*) (*H, arrow*). *I* and *J*, many H9APP WT NPCs expressed Tbr2, an intermediate basal progenitor cell marker. *K* and *L*, furthermore, a subset of cells (≈10%) expresses the mature neural marker tau and (*M, N,* and *P*) exhibits extensive neurite outgrowth. *O*, in contrast, less than 1% of the cells expressed the astrocyte marker GFAP.

expression of Pax6 (Fig. 2*U*) and minimal expression of TUJ (<2.5%, *W*). In contrast, between 60 and 75% of cells in APP-ESC colonies expressed TUJ, representing about a 30-fold increase in neural differentiation that was highly significant (ANOVA, $p = 0.001$, Fig. 2, *O, S,* and *Z*). No difference in TUJ expression between mutant or wild-type APP-ESC clones was detected (ANOVA, $p = 0.1$). We did, however, observe that the degree of differentiation varied across and even within colonies. For example, in some regions, clusters of cells coexpressed both TUJ and Pax6 immunoreactivity, likely representing more immature neurons or neural progenitors (Fig. 2, *M–P*). In contrast, other regions, even within the same colony, exhibited large uniform areas of TUJ-immunoreactive cells that were Pax6-negative, likely representing more mature neurons (Fig. 2,

FIGURE 2. **APP overexpression drives rapid and robust neuronal differentiation of H9 and HUES7 hESCs.** Despite maintenance in standard hESC media, APP overexpressing H9 (*A–D*) and HUES7 (*E–H*) clones spontaneously differentiate, forming large numbers of neural rosettes that express the early neural marker nestin (*A, D, E,* and *H; red*). The inner lumens of these rosettes are also immunoreactive for the apical marker ZO-1 (*C, D, G,* and *H; green*). *I–L*, in contrast, control H9 colonies show almost no nestin-positive cells, and ZO-1 labeling is restricted to the cell membrane. *M–P*, H9 APP WT rosettes also express the neural markers PAX6-positive and TUJ-positive, and uniform patches of more mature PAX6-negative/TUJ-positive NPCs are also observed (*Q–T*). *U–X*, control H9 cells, by comparison, express neither PAX6 nor TUJ. *Y*, qPCR shows that Sox2, nestin, and Tbr2 neural progenitor transcripts are up-regulated in both H9 APP WT and H9 APP Swe clones *versus* control H9 cells. GFAP, a marker of both neural progenitors and astrocytes, is also elevated in both clones, as is the neural transcript TUJ. The oligodendrocyte transcription factor Olig2 is increased in H9 APP WT clones and down-regulated in H9 APP Swe clones. *Z* and *Z'*, although almost no H9 cells express nestin or TUJ, these markers are expressed by 83 and 63% of H9 APP WT cells and by 79 and 65% of H9 APP Swe cells, respectively (*, $p < 0.05$).

Q–T). Importantly, each of these phenotypes was observed within just 4–6 days of manual passaging, representing an exceedingly rapid progression of neural differentiation.

To further characterize the spontaneous differentiation of our APP hESC lines, we performed qPCR analysis of several important transcripts. In accordance with our immunofluorescence data, we detected a consistent up-regulation of the pro-neural transcripts Sox2, nestin, and Tbr2 by 3–5-fold, 2-fold, and 2–3-fold, respectively (Fig. 2*Y*). GFAP, which is expressed by both astrocytes and neural precursors, was also significantly increased, as was the more mature neural marker TUJ. Interestingly, expression of the oligodendroglial transcript Olig2 was only up-regulated in wild-type APP-hESC clones (Fig. 2*Y*).

To determine whether APP expression was present within differentiating cells, we examined the coexpression of APP and TUJ (Fig. 3, *A–H*). As shown, APP immunoreactivity is clearly detected within rosette-like structures (Fig. 3*A*, *arrow*) and TUJ+ neurons (*H*, *arrow*). Next, we investigated whether any of the cells in APP-overexpressing cultures expressed more mature neuronal markers, such as the microtubule-binding protein tau. Within 5 days of manual passaging, 5–10% of cells were immunoreactive for tau (Fig. 3, *K* and *L*). Notably, these tau-immunolabeled cells also exhibited long, thin, polarized, and branching processes typical of neurons (Fig. 3, *K* and *L*). Far fewer cells expressed the astrocytic marker GFAP (0.5–1%), indicating that a minority of neural progenitors become astrocytes, whereas the majority express neuronal markers (Fig. 3*O*).

Interestingly, APP-hESC colonies display a wide range of neural differentiation. Although many cells coexpress the neural progenitor markers nestin+ and Sox2+, cells that coexpress Sox2 and TUJ or nestin and TUJ were also observed (supplemental Fig. 1). More mature cells that expressed TUJ alone were also observed frequently. These findings suggests that the rapid rate of differentiation occurring in APP-hESC clones may blur the traditional boundaries between earlier (Sox-2, nestin) and later (TUJ) neural markers. Nevertheless, differentiation appears to proceed so that more mature neuronal morphology and tau expression is also observed within just 5 days of passaging (Fig. 3, *K* and *L*).

To determine whether changes in notch signaling may play a role in the observed neural differentiation, we examined the expression of a primary downstream target of notch: Hes1 (22). Our qPCR results revealed no differences in Hes1 expression between control H9 cells and the APP-hESC clones (data not shown), suggesting that altered notch signaling is not involved in the observed differentiation phenotype.

We also observed that APP-overexpressing hESC lines spontaneously organized to produce two different types of tubular structures. Although the smaller tubular structures labeled with neural lineage markers and ZO-1 and appeared morphologically identical to ESC-derived neural rosettes (Fig. 2, *A–H*), our APP-expressing clones also produced large tubular structures that did not express neuronal markers (Fig. 1*E*). Instead, these more rarely occurring tubular structures stain positive for brachyury, and qPCR confirmed increased expression of brachyury mRNA (supplemental Fig. 2). Staining for the actin smooth muscle protein, a more mature mesodermal marker, was also observed within a few cells within these tubular struc-

tures (supplemental Fig. 2*D*). Interestingly, qPCR measurements of GATA-4, an endodermal-specific transcript, were significantly reduced in APP-hESC clones.

Taken together, these results show that overexpression of APP promotes differentiation into the neural lineage and may to a lesser extent also drive mesodermal differentiation although preventing endodermal differentiation. This also highlights the fact that the fate choice induced by APP overexpression is not a random event and drives differentiation toward specific lineages.

Effects of APP Overexpression on Key APP-processing Enzymes—To begin to investigate the mechanism by which APP overexpression drives neural differentiation, we examined the enzymes and cleavage products involved in APP processing. α-Secretase activity is mediated via either ADAM10 or ADAM17, both of which we found to be expressed in hESCs. However, no differences in either mature or immature ADAM10 or ADAM17 were detected (supplemental Fig. 3, *A–D*, ANOVA, $p = 0.5$ for immature and $p = 0.74$ for mature ADAM10, $p = 0.89$ for immature and $p = 0.73$ for mature ADAM17). In contrast, β-secretase expression was significantly elevated in APP-hESC cell lines (supplemental Fig. 3, *E* and *G*, ANOVA, $p = 0.0065$). This observation is consistent with previous reports that BACE1 levels are elevated in sporadic AD patients (23) and transgenic AD mice (24, 25). In concordance with elevated BACE1 expression, we also observed a significant up-regulation of the APP C-terminal fragments (supplemental Fig. 3, *F* and *H*, ANOVA, $p = 0.0001$).

To determine whether components of the γ-secretase complex are altered in the APP hESC lines, we examined the expression of presenilin 1 (PS1), presenilin 2 (PS2), and nicastrin. The presenilins form the catalytic core of the γ-secretase complex, whereas nicastrin is implicated in substrate binding (26, 27). Interestingly, we found a strong trend toward reduced expression of both PS1 (supplemental Fig. 3, *I* and *K*) and nicastrin (supplemental Fig. 3, *J* and *L*) in APP-hESC clones, although these differences failed to reach significance (ANOVA, $p = 0.06$, $p = 0.12$, respectively). Expression of full-length PS2 was extremely low in all hESC lines. Furthermore, the catalytically active C-terminal fragment of PS2 was undetectable in both APP and control H9 cells, suggesting that there is little, if any, PS2 activity in hESCs (supplemental Fig. 3*M*). Taken together, we found no change in α-secretase, an increase in β-secretase with a subsequent accumulation of APP C-terminal fragments, and trends toward reduction in γ-secretase components.

To examine $A\beta$ levels in control and APP-hESC clones, we also performed a sensitive sandwich ELISA capable of detecting as little as 0.6 pmol/liter $A\beta$. However, neither $A\beta40$ nor $A\beta42$ were detected (data not shown), suggesting that production of $A\beta$ by hESCs is minimal.

Soluble APP Drives Robust Neural Differentiation of Unaltered H9 hESCs—The preferential differentiation of APP-hESC clones into neural cells could be triggered by one of the several cleavage products of APP proteolysis. In addition to $A\beta$, APP cleavage leads to the production of secreted soluble APP α and β fragments (sAPPs) and AICD. Previous studies have shown that sAPPα can exhibit growth factor-like properties and can even increase the proliferation of adult neural progenitor cells
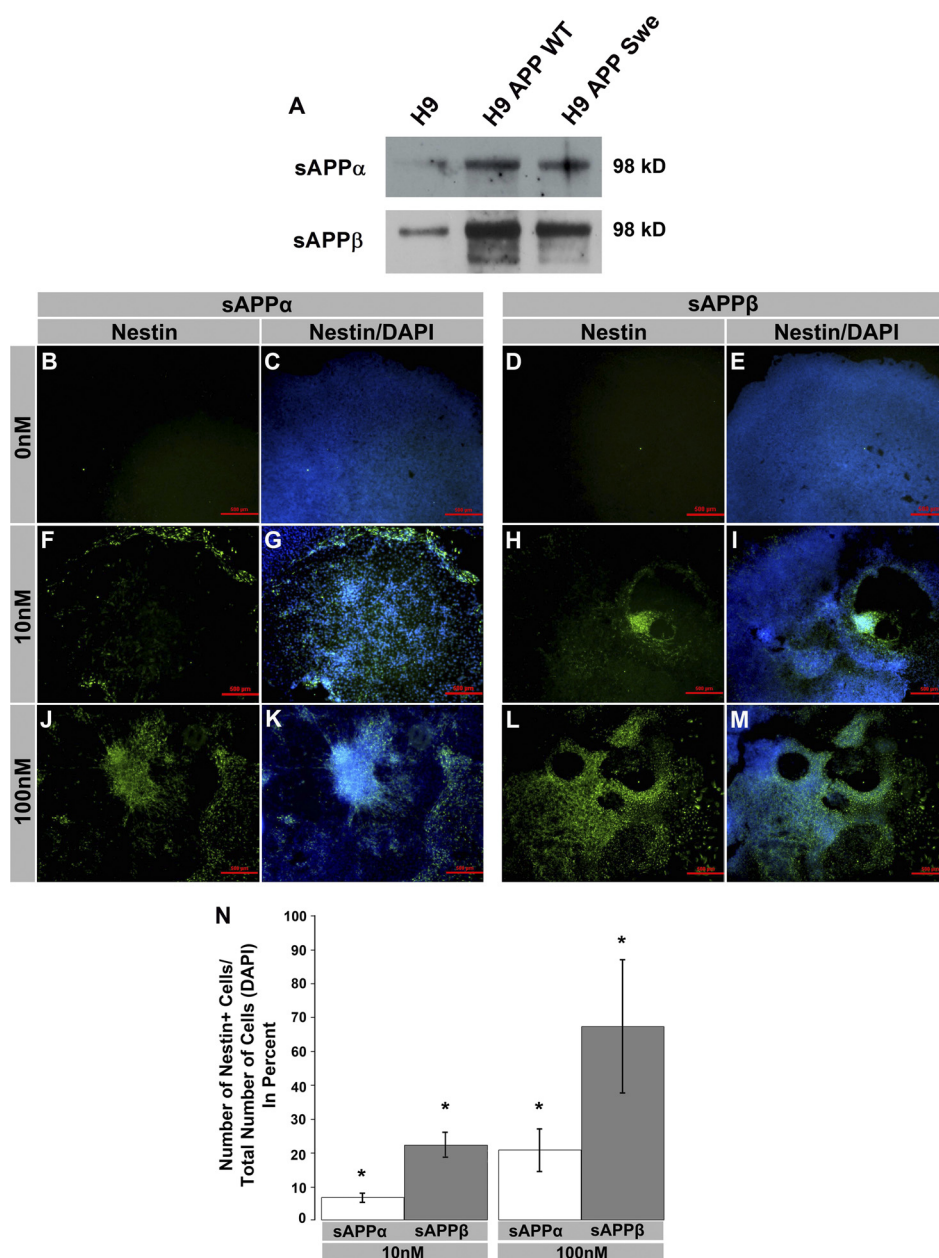
FIGURE 4. **Recombinant sAPPα and β mimic the effects of APP overexpression by inducing rapid neural differentiation of H9 hESCs.** *A*, collected media supernatant from APP-ES cell clones have robustly elevated levels of sAPPα and even more sAPPβ protein. *B–E* and *N*, H9 cultures treated with vehicle (0 nM) show less than 1% nestin immunoreactivity. *F–I*, in contrast, addition of 10 nM recombinant sAPPα or β protein induces significant differentiation and nestin expression. *J–M*, treatment of H9 cultures with 100 nM sAPPα or β protein induces further neural differentiation. *N*, quantification reveals that 6% of cells treated with 10 nM sAPPα and 22% of those treated with 10 nM sAPPβ express nestin. These percentages increased in a dose-dependent manner with 100 nM sAPPα yielding 20%, and 100 nM sAPPβ yielding 57% nestin-positive cells (*, $p < 0.05$). Thus, sAPPβ appears to be considerably more potent than sAPPα at inducing neural commitment.

in vitro (10). Hence, we examined the relative amounts of sAPPα and sAPPβ secreted into the media of APP-expressing and control H9 cells. After enrichment and immunoprecipitation with an antibody directed against the N terminus of APP (22C11), we performed a Western blot analysis with sAPPα- and sAPPβ- specific antibodies. As shown, we detected a robust increase in sAPPα and an even more pronounced elevation of sAPPβ within the conditioned media of APP-hESC clones (Fig. 4*A*).

To further investigate whether increased sAPP secretion plays a role in the neural differentiation of APP hESCs, we treated control H9 hESC cultures with recombinant sAPPα or sAPPβ protein. 0 nM, 1 nM, 10 nM, or 100 nM of each recombinant protein was added to H9 cells growing in mTeSR® media, and protein-spiked media was replaced daily for 5 days to mimic the time course of neural differentiation observed in our APP-ESC clones. Cultures were then fixed and analyzed by immunofluorescent microscopy. Addition of 1 nM sAPPα or β produced no detectable effects on neural differentiation, and the expression of nestin was comparable with the control (data not shown). In contrast, addition of 10 nM sAPPα induced an increase of 6.57% (Fig. 4, *F*, *G*, and *N*), and addition of 10 nM
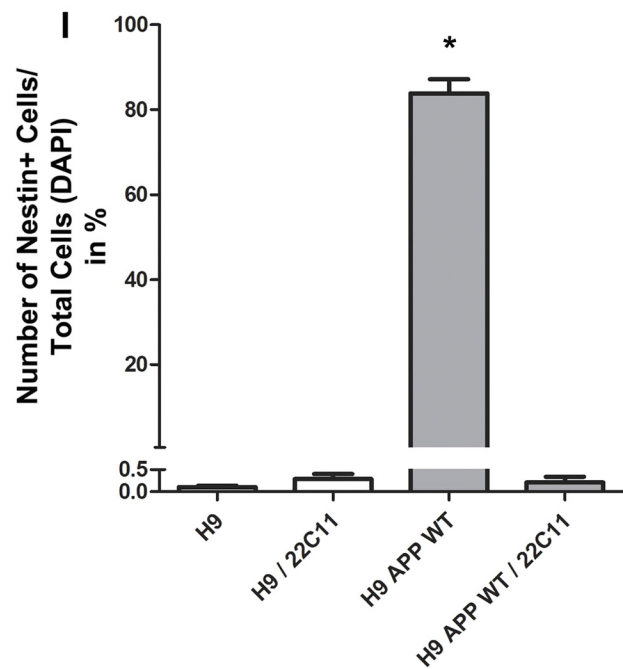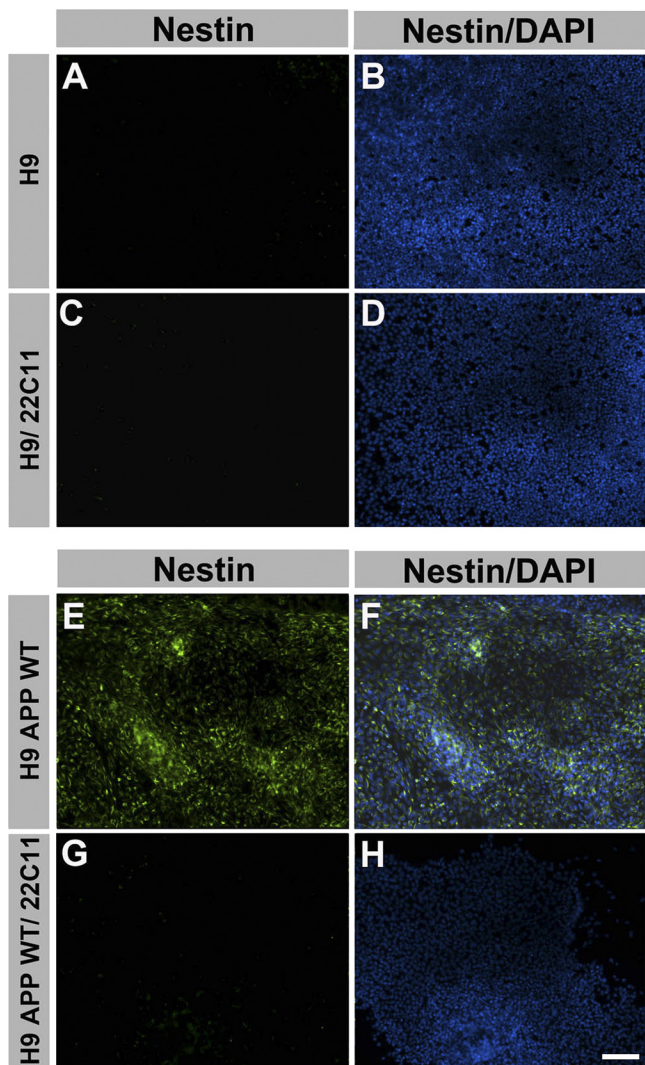
sAPPβ induced a greater increase of 22.1% in nestin-positive cells (*H*, *I*, and *N*). In H9 cell cultures treated with 100 nM sAPPα the amount of nestin-positive cells increased to 20.6% (Fig. 4, *J*, *K*, and *N*), whereas treatment with 100 nM sAPPβ resulted in 57.1% nestin-immunoreactive cells (*L–N*). The increase in nestin-positive cells with recombinant sAPPα and sAPPβ treatment was highly significant and dose-dependent (ANOVA, $p = 0.0006$). In addition to the marked effect of sAPP treatment on neural differentiation, we observed similar three-dimensional structures to those observed in APP transgenic lines (Fig. 4, *I*, *K*, and *M*), although these structures were less organized and occurred less frequently. Interestingly, we observed tau-immunoreactive neurons after 5 days in APP-hESC cultures (Fig. 3, *K* and *L*), whereas few or no tau-positive cells are detected in hESC treated for 5 days with recombinant sAPPs (supplemental Fig. 4, *A* and *B*). However, by 12 days of sAPP treatment, many more tau-immunoreactive cells are observed especially in sAPPβ-treated cultures (supplemental Fig. 4, *C* and *D*). These data suggest that although sAPP treatment closely mimics APP-overexpression, neuronal maturation appears to proceed at a somewhat slower rate in sAPP-treated cultures. These differences may be explained by different secondary and tertiary structures of sAPP recombinant protein generated in *Escherichia coli versus* the more physiologic glycosylation and folding that likely occurs in APP-overexpressing hESCs. Another intriguing possibility is that the localized cell-based production and secretion of sAPPs provides a more organized gradient that better mimics developmental programs than does bathing cells in recombinant protein.

Antibody Blocking Experiments Confirm That sAPPs Drive Neural Differentiation of APP-hESCs—To determine whether neural differentiation of APP-hESCs is mediated via sAPPα and sAPPβ, we used an N-terminal-specific antibody (22C11) to block sAPP activity. Manually passaged H9 APP WT and H9 control hESCs were treated with 22C11 over the course of 5 days. During this time frame, we typically observe massive neural commitment of the APP-ES cell clones. Untreated H9 hESC cells behaved normally, showing no signs of differentiation (Fig. 5*A*, *B*, and *I*), whereas untreated H9 APP WT cells differentiated rapidly with 83% of the cells expressing nestin after 5 days (*E*, *F*, and *I*). In contrast, treatment with 22C11 completely abolished neural differentiation of H9-APP WT hESCs (Fig. 5, *G*, *H*, and *I*) and had no effect on H9 control cells (*C*, *D*, and *I*). These experiments clearly demonstrate that sAPP peptides mediate much, if not all, of the spontaneous neural differentiation observed in APP-hESC clones. Taken together, our results strongly indicate that soluble APP, and especially sAPPβ, has a significant influence on neural fate.

FIGURE 5. **Neural differentiation of APP-hESCs is prevented by treatment with an antibody that binds sAPPα and β.** *A–D* and *I*, H9 control cultures treated with vehicle or the N-terminal specific antibody, 22C11, remain undifferentiated. *E–H* and *I*, in contrast, vehicle-treated H9 APP WT cells rapidly differentiate into nestin-positive NPCs, whereas 22C11 antibody treatment prevents differentiation. Thus, sAPPs mediate neural differentiation of hESCs (*, $p < 0.05$). *Scale bar = 350 μm.*

DISCUSSION

In this study, we generated hESC lines that stably overexpress wild-type or mutant APP to provide a novel human cell-based approach to examine the molecular and cellular pathways that underlie the development of AD. Interestingly, during the characterization of these APP-expressing lines, we observed that these cells rapidly, robustly, and spontaneously differentiate toward a neural phenotype. Importantly, this phenomenon was not cell line-specific, as we observed the same response in APP-expressing HUES7 clones (Fig. 2, *E–H*). To determine the underlying mechanism by which APP drives neural differentiation, we examined APP proteolysis and the roles of various APP-derived fragments in neural differentiation. Our results demonstrate that two secreted APP-derived soluble peptides (sAPPα and sAPPβ) drive neural differentiation of hESCs in a concentration-dependent manner.

Previous studies showed that sAPPα can promote neuronal survival and neurite outgrowth (28–30). This trophic-like activity has also more recently been shown to promote the proliferation of adult rodent subventricular zone progenitors (31). However, the potential influence of APP and sAPP fragments on human ES cells has thus far remained largely unexplored. Intriguingly, although sAPPα has been shown by others to mediate much of the neurotrophic properties of sAPPs, here we report the novel findings that sAPPβ is more potent at inducing hESC neural differentiation (Fig. 4). Importantly, our studies have also uncovered a straightforward and reproducible method to generate large numbers of neural cells from hESCs within just 5–6 days. Current protocols, in contrast, typically require 21 or more days to produce an equivalent yield of neural cells (32).

To understand why sAPPβ more readily drives differentiation of hESCs than sAPPα, the downstream targets of sAPP signaling will need to be identified. Toward that end, a recent study found that sAPPβ can regulate the transcription of transthyretin and Klotho genes in the absence of full-length APP or APLP1 expression (33). The mechanism by which sAPPβ modulates gene transcription remains unknown. However, the study by Li *et al.* provides some of the first evidence that sAPPs can differentially modulate specific gene targets (33). Future studies will aim to unravel the specific transcriptional targets of sAPPs that mediate our observed effects on hESC differentiation.

Although our data clearly demonstrate that overexpression of APP can drive neural differentiation of hESCs, a recent examination of mouse ESCs suggests that deletion of APP and its two homologues (APLP1 and APLP2) does not alter differentiation (34). Two possible explanations may account for this apparent difference. First, our observed neural induction occurs spontaneously in ES media and in the absence of additional factors that can promote neural differentiation. In contrast, Bergmans *et al.* (34) employed a standard neural differentiation protocol, generating embryoid bodies supplemented with retinoic acid and later adding N2 and B27 supplements to further drive differentiation. It is likely that more subtle physiological effects of APP deletion on neural differentiation can be readily overcome by the use of strong neural inducing agents

such as retinoic acid. Second, although our experiments utilized hESCs, Bergmans *et al.* (34) studied mouse knockout ESCs. It is possible that in man, modulation and proteolysis of APP plays a more significant role in the development and differentiation of neurons than in mice. In support of this notion, functional differences exist between several human and mouse proteins implicated in AD, including APP, tau, and ApoE (35–38). Clearly, to more fully address the physiological function of APP in human cells, knockdown and knockout studies in hESCs will be needed.

In our cell model, we identified an increase in soluble secreted fragments of APP as the major mechanism underlying spontaneous neural differentiation of APP-ESC clones. Intriguingly, although the majority of studies have focused on the trophic activity of sAPPα in neuronal growth, we found instead that sAPPβ is the more potent of the two at driving neural differentiation. This is a significant finding because much effort has been expended in the development of drugs aimed at reducing or abolishing β-secretase activity (39, 40). Although inhibition of β-secretase would reduce levels of Aβ, our data indicate that β-secretase activity may be involved in neural induction. Whether or not sAPPβ can also modulate adult neurogenesis in a parallel manner to sAPPα remains to be determined.

Interestingly, a recent study showed that soluble and fibrillar Aβ could promote hESC proliferation, whereas treatment of hESCs with a β-secretase inhibitor decreased proliferation and increased nestin expression (5). We argued that a shift in APP processing from amyloidogenic (β-secretase-mediated) to non-amyloidogenic (α-secretase-mediated) may drive differentiation. Our experiments would argue against this conclusion, as we find that sAPPβ drives robust neural differentiation (Fig. 4). We also observed no differences in the degree of neural induction between wild-type and Swedish mutant APP clones despite the fact that the Swedish mutation increases BACE1 cleavage and decreases α cleavage of APP. One possible explanation for this difference is that BACE1 inhibition would lead to altered processing of many other developmentally relevant BACE1 substrates. For example, a recent study identified several proteins critically involved in neurodevelopment as being substrates for BACE1 cleavage (41). Most notable among these was the notch ligand Jagged-1, which has itself been shown to drive neural differentiation of ESCs (42). Thus, the effects of BACE inhibition on neural differentiation likely occur independent of altered APP processing.

A further significant finding of our study was that proteins that comprise the γ-secretase complex are present at very low levels in hESCs. This finding suggests that γ-secretase-mediated cleavage of APP may not be necessary for neural induction. Consistent with this result, we were unable to detect either Aβ40 or 42 productions by hESCs despite the use of a highly sensitive ELISA (data not shown). Interestingly, another group recently showed that AICD interacts with TAG1 and negatively modulates neurogenesis through FE65 in NPCs (11). This report supports our finding that subsequent interactions and pathways involving γ-secretase-mediated APP cleavage products are not the predominant driver of neural induction.

Studies of patients and transgenic AD models support the notion that altered APP expression or processing may modu-

late adult neurogenesis. However, the data remain conflicting. Although some groups have reported impaired neurogenesis in animal models of AD (43, 44), a converse phenotype has been seen by others. For example, studies of AD patients and mouse models that overexpress the human APP gene have revealed an increase in adult neurogenesis (45, 46). These latter findings clearly fit with our current study and suggest that in patients altered APP processing may well lead to increased neurogenesis, although this change is clearly unable to compensate for the widespread neuronal dysfunction that occurs with the disease.

By generating and examining hESC lines overexpressing either wild-type or mutant forms of APP, we identified a previously unknown role for APP and sAPPs in the neuronal differentiation of hESCs. We also show that the proneural activity of sAPPβ can be readily exploited to generate large numbers of neural cells from hESCs within just 5–6 days as compared with the 21+ days required by current protocols (32). These APP-overexpressing lines will likely provide a valuable platform for the further dissection of both AD pathogenesis and APP cell biology in a human context. Future studies will be needed to expand our understanding how sAPPβ promotes neural differentiation. For example, it will be critical to identify the downstream targets and signaling pathways activated by sAPPβ in hESCs. By enhancing our understanding of the physiological functions of APP and its role in stem cell differentiation, these studies may also help to guide the development of novel approaches to treat AD.

REFERENCES

1. Querfurth, H. W., and LaFerla, F. M. (2010) *N. Engl. J. Med.* **362,** 329–344
2. Glabe, C. C. (2005) *Subcell. Biochem.* **38,** 167–177
3. Young-Pearse, T. L., Bai, J., Chang, R., Zheng, J. B., LoTurco, J. J., and Selkoe, D. J. (2007) *J. Neurosci.* **27,** 14459–14469
4. Herms, J., Anliker, B., Heber, S., Ring, S., Fuhrmann, M., Kretzschmar, H., Sisodia, S., and Müller, U. (2004) *EMBO J.* **23,** 4106–4115
5. Porayette, P., Gallego, M. J., Kaltcheva, M. M., Bowen, R. L., Vadakkadath Meethal, S., and Atwood, C. S. (2009) *J. Biol. Chem.* **284,** 23806–23817
6. Chow, V. W., Mattson, M. P., Wong, P. C., and Gleichmann, M. (2010) *Neuromolecular Med.* **12,** 1–12
7. De Strooper, B., and Annaert, W. (2000) *J. Cell Sci.* **113,** 1857–1870
8. Gakhar-Koppole, N., Hundeshagen, P., Mandl, C., Weyer, S. W., Allinquant, B., Müller, U., and Ciccolini, F. (2008) *Eur. J. Neurosci.* **28,** 871–882
9. Perez, R. G., Zheng, H., Van der Ploeg, L. H., and Koo, E. H. (1997) *J. Neurosci.* **17,** 9407–9414
10. Caillé, I., Allinquant, B., Dupont, E., Bouillot, C., Langer, A., Müller, U., and Prochiantz, A. (2004) *Development* **131,** 2173–2181
11. Ma, Q. H., Futagawa, T., Yang, W. L., Jiang, X. D., Zeng, L., Takeda, Y., Xu, R. X., Bagnard, D., Schachner, M., Furley, A. J., Karagogeos, D., Watanabe, K., Dawe, G. S., and Xiao, Z. C. (2008) *Nat. Cell Biol.* **10,** 283–294
12. Kamal, A., Almenar-Queralt, A., LeBlanc, J. F., Roberts, E. A., and Goldstein, L. S. (2001) *Nature* **414,** 643–648
13. Kamenetz, F., Tomita, T., Hsieh, H., Seabrook, G., Borchelt, D., Iwatsubo, T., Sisodia, S., and Malinow, R. (2003) *Neuron* **37,** 925–937
14. Cao, X., and Südhof, T. C. (2001) *Science* **293,** 115–120
15. Cao, X., and Südhof, T. C. (2004) *J. Biol. Chem.* **279,** 24601–24611
16. Haas, C., Hung, A. Y., Citron, M., Teplow, D. B., and Selkoe, D. J. (1995) *Arzneim. Forschung* **45,** 398–402
17. Tanaka, S., Shiojiri, S., Takahashi, Y., Kitaguchi, N., Ito, H., Kameyama, M., Kimura, J., Nakamura, S., and Ueda, K. (1989) *Biochem. Biophys. Res. Commun.* **165,** 1406–1414
18. Lahiri, D. K., and Ge, Y. W. (2004) *Ann. N.Y. Acad. Sci.* **1030,** 310–316
19. Miragall, F., Krause, D., de Vries, U., and Dermietzel, R. (1994) *J. Comp. Neurol.* **341,** 433–448
20. Wen, J., Hu, Q., Li, M., Wang, S., Zhang, L., Chen, Y., and Li, L. (2008) *Neuroreport* **19,** 413–417
21. Sessa, A., Mao, C. A., Hadjantonakis, A. K., Klein, W. H., and Broccoli, V. (2008) *Neuron* **60,** 56–69
22. Ohtsuka, T., Ishibashi, M., Gradwohl, G., Nakanishi, S., Guillemot, F., and Kageyama, R. (1999) *EMBO J.* **18,** 2196–2207
23. Li, R., Lindholm, K., Yang, L. B., Yue, X., Citron, M., Yan, R., Beach, T., Sue, L., Sabbagh, M., Cai, H., Wong, P., Price, D., and Shen, Y. (2004) *Proc. Natl. Acad. Sci. U.S.A.* **101,** 3632–3637
24. Zhao, J., Fu, Y., Yasvoina, M., Shao, P., Hitt, B., O'Connor, T., Logan, S., Maus, E., Citron, M., Berry, R., Binder, L., and Vassar, R. (2007) *J. Neurosci.* **27,** 3639–3649
25. Zhang, X. M., Cai, Y., Xiong, K., Cai, H., Luo, X. G., Feng, J. C., Clough, R. W., Struble, R. G., Patrylo, P. R., and Yan, X. X. (2009) *Eur. J. Neurosci.* **30,** 2271–2283
26. Steiner, H., Fluhrer, R., and Haass, C. (2008) *J. Biol. Chem.* **283,** 29627–29631
27. Steiner, H., Winkler, E., and Haass, C. (2008) *J. Biol. Chem.* **283,** 34677–34686
28. Araki, W., Kitaguchi, N., Tokushima, Y., Ishii, K., Aratake, H., Shimohama, S., Nakamura, S., and Kimura, J. (1991) *Biochem. Biophys. Res. Commun.* **181,** 265–271
29. Milward, E. A., Papadopoulos, R., Fuller, S. J., Moir, R. D., Small, D., Beyreuther, K., and Masters, C. L. (1992) *Neuron* **9,** 129–137
30. Mattson, M. P., Cheng, B., Culwell, A. R., Esch, F. S., Lieberburg, I., and Rydel, R. E. (1993) *Neuron* **10,** 243–254
31. Gralle, M., and Ferreira, S. T. (2007) *Prog. Neurobiol.* **82,** 11–32
32. Chambers, S. M., Fasano, C. A., Papapetrou, E. P., Tomishima, M., Sadelain, M., and Studer, L. (2009) *Nat. Biotechnol.* **27,** 275–280
33. Li, H., Wang, B., Wang, Z., Guo, Q., Tabuchi, K., Hammer, R. E., Südhof, T. C., and Zheng, H. (2010) *Proc. Natl. Acad. Sci. U.S.A.* **107,** 17362–17367
34. Bergmans, B. A., Shariati, S. A., Habets, R. L., Verstreken, P., Schoonjans, L., Müller, U., Dotti, C. G., and De Strooper, B. (2010) *Stem. Cells.* **28,** 399–406
35. Ivanova, M. I., Sawaya, M. R., Gingery, M., Attinger, A., and Eisenberg, D. (2004) *Proc. Natl. Acad. Sci. U.S.A.* **101,** 10584–10589
36. Spillantini, M. G., and Goedert, M. (1998) *Trends Neurosci.* **21,** 428–433
37. Kampers, T., Pangalos, M., Geerts, H., Wiech, H., and Mandelkow, E. (1999) *FEBS Lett.* **451,** 39–44
38. Brion, J. P., Smith, C., Couck, A. M., Gallo, J. M., and Anderton, B. H. (1993) *J. Neurochem.* **61,** 2071–2080
39. Evin, G., and Kenche, V. B. (2007) *Recent. Pat. CNS Drug Discov.* **2,** 188–199
40. Wolfe, M. S. (2008) *Curr. Alzheimer Res.* **5,** 158–164
41. Hemming, M. L., Elias, J. E., Gygi, S. P., and Selkoe, D. J. (2009) *PLoS ONE* **4,** e8477
42. Ramasamy, S. K., and Lenka, N. (2010) *Mol. Cell. Biol.* **30,** 1946–1957
43. Haughey, N. J., Nath, A., Chan, S. L., Borchard, A. C., Rao, M. S., and Mattson, M. P. (2002) *J. Neurochem.* **83,** 1509–1524
44. Haughey, N. J., Liu, D., Nath, A., Borchard, A. C., and Mattson, M. P. (2002) *Neuromolecular Med.* **1,** 125–135
45. Jin, K., Galvan, V., Xie, L., Mao, X. O., Gorostiza, O. F., Bredesen, D. E., and Greenberg, D. A. (2004) *Proc. Natl. Acad. Sci. U.S.A.* **101,** 13363–13367
46. Ziabreva, I., Perry, E., Perry, R., Minger, S. L., Ekonomou, A., Przyborski, S., and Ballard, C. (2006) *J. Psychosom. Res.* **61,** 311–316